International Journal of Scientific Engineering and Applied Science (IJSEAS) – Volume-6, Issue-9, September 2020
ISSN: 2395-3470
www.ijseas.com

Analysis of New Robotic Cylinder Hemming System Used In Metal Edge Folding of Automobile Doors Using FEM

Ozdogan Karacali[1], Gulcan Samar[1], Oguz Borat[2] and Osman Yazicioglu[2]
[1] Istanbul University-Cerrahpasa, Engineering Faculty, Istanbul, 34320 Turkey
[2*] Istanbul Commerce University, Engineering Faculty, Istanbul, 34840 Turkey

Abstract

Roller hemming technology is a new production engineering technique that has many advantages in terms of cost and time. Hemming is a forming process in which the edges of the sheet metal plate in automotive doors and panels fold over another piece to fit tightly. Hemming is the last of the final stage operations in the assembly of automotive door parts. As such, it is critical on the performance and quality of assembled vehicles. Hemming used to tie two sheet metal pieces together, or to enhance a smooth edge appearance, rather than a burr-shaved one. However, it is not always easy to design the association of sheet metal sheets in the same plane and influenced by the mechanical properties of the material of the curling part. The main problems in the automotive industry occur when bending aluminum alloys. There is very limited literature that scientifically explains the stresses that occur during the hemming process and the transformation in the material. In this study, using the finite element method LS-DYNA explicit analysis, the stress and von Mises criteria that cause edge cracks to occur in AA6062-T4 aluminum plates investigated. In this research, the stresses that occur during the hemming process examined the cracks on the edge due to the sensitivity of the strain to break. To avoid this problem, and due to the limitations of traditional flanging and hemming technologies, the flange radius and hemming cylinder were studied when working with aluminum alloys. The dies and tools used for the hemming process designed based on experience and long and expensive mold trials. Ensuring and maintaining the correct product quality is possible through several trial-and-error processes. In this study, experimental research conducted to compare the results between simulation and experiment. Finite element analysis (FEA) seen in this study where the robotic cylinder hemming process shortened the trial and error process.

Keywords: Hemming, Sheet Metal Forming, Fasteners, Automobile Doors, Finite Element Method.

1. Introduction

Bending operations performed using punch die tooling. The two common bending methods and associated tooling V-bending and edge bending. Hemming involves bending the edge of the sheet over on itself, in more than one bending step. Toeniskoetter [1,2] received some patents by hemming regarding the machine and apparatus. The main goal of the current study is to develop a methodology to simulate the hemming process with acceptable accuracy and efficiency. Previous works mostly focus on hemming. La Mout et al. [3,4] used finite element simulation of the roll hemming process of an Al-Mg alloy [Le Maoût 2006]. Muderrisoglu et al. [5] analysis effects of hemming roll-in / out flange parameters on 1050 aluminum alloy. Zhang et al. [6,7] table top hemming warp and recoil mechanism examined. Livatyali et al. [8] studied the effects of flange and hemming parameters on tabletop hemming quality through simulation and experiments. Studies in 2000 concerned the flange pattern radius, pre - hem path, pre-hem stroke and end-hemming force on warp/recoil and roll-in/out for flat-surface straight-edged hemming. In 2002, the most accurate and effective finite element method and Commercial Code for flat flange operation was determined. In 2004, defects in hemming of soft steel sheets with flat surface convex edge geometry, forming rolls and warps experimentally investigated. The study showed that the effect of stroke radius on roll-in/out was relatively stronger than other parameters. Bagheri [9,10] researched rubber-assisted parametric pre-hemming process and Lin et al. [11,12] hemming presented maximum surface plastic strain as the breaking criterion. Le Port et al. [13] evaluated some surface defects on the automobile panels after flanging affected by different materials, flanging length, corner radius,

and flanging radius. However, cyclic hardening parameters were determined by simple shear [14] and cyclic bending [15] tests. Wanintradul [16] investigated hemming covered the warp and recoil mechanism. Zhang et al. [17] hemming presented maximum surface strain as the refractive criterion. Thuillier [18] focused on the finite element simulation of Table - Top hemming and cylinder hemming of an Al–Mg alloy in roll-in/out.
This paper presents a study of the cyclic hardening behavior of roller hemming in aluminum alloy sheets. First, the finite cylinder rolling element model was established. Special sample holder and modified single-axis samples used for single-axis tension and compression tests. Combined hardening parameters obtained from single axis tension and compression tests verified by pre-hemming in/out datum. Finally, the cyclic hardening behavior of roller hemming of aluminum alloy studied based on simulation results.

2. Materials and Method

Roll hemming simulation classified as three steps: flanging, pre-hemming, and final hemming. First, a flat outer panel with a 90 ° flange angle bent. Then the outer panel turned to 0°. ABAQUS / EXPLICIT is used to simulate the cylinder hemming process. A flat panel with straight edges used in this simulation. Flat surface-flat edge specimen has a length of 200 mm and width equal to 60 mm before flanging. The inner cavity is 200 mm long and 42 mm wide.
The bending area is the maximum deformed area. The nets are refined to a minimum size of 0.2 mm (Figure 1). The flange area is the folding area. The Nets are refined to a minimum size of 1 mm. The transition and very slightly deformed regions are rough-knit. Ultimately, there are 17,956 elements anointed to the outer space. While the inner cavity roughly knitted into the rough, the cylinder slightly deformed during the hemming process (Figure 1).

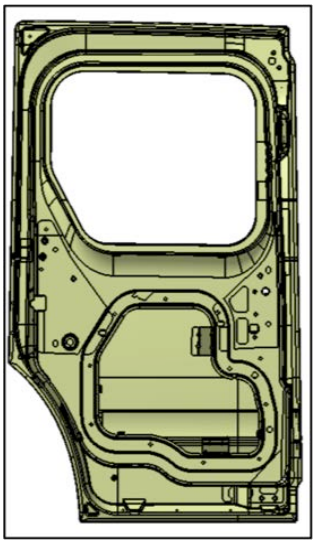

Figure 1. View of car door body model.

Based on practical considerations, a discrete scheme chosen to estimate the formatting mechanism of the samples, the FEM procedure expressed as:
The LS-DYNA originally used to simulate the problem, taking into account its mechanical aspect. With this iterative process, an estimate of the total average force applied to the metal plate portion is calculated, and then, PAM-STAMP2G brought in as an input charge for simulation of the deformation process made using a special code. A quantitative match of the force parameter in question followed by the adjustment of the peak value of the pressure or force pulse, which acts as an input in the Pam-stamp.
The critical point focuses on how this force value is transferred to a deformation code as an input charge, i.e., as a force-time curve. Thus, the proposed set of experiments not considered as a benchmarking problem to assess the feasibility of the iteration scheme, but to obtain rough trends regarding the variables studied, it referred to as: a) Global shape of the samples. b) Evolution of deformation model. c) Stress levels present in samples.

3. Analysis

The Robot cylinder edge folding process is a forming process that can be adapted to the factory production line used in the automotive industry. In general, this process was preferred in automobile body manufacturing, resulting in a robotic system structure with more precise processing surfaces than the classic clamping and hemming process. This structure was preferred because the materials we prefer in the car doors and bodywork with sloping surface quality will create deformations such as wrinkles and stretching back after the process. Instead of the mold and transport robot used in the classical methods, there was a reduction in the process with a single robot arm.

The aim of this study is to show that the steps of hemming, mastic and laser curing process proceed in a complementary manner with the robot arm attached to a single robot. In order to perform these complementary steps, some parameters that also affect process quality need to be determined. The effects of the placement of the robot arm on the workpiece analyzed numerically and the optimal processing parameters were determined.

Also important here are the body fittings used as well as the dimensions and material structure of the inner and outer panel. Although there is no effect on the internal and external panels installed during the hemming process, if the placement of the used fittings not performed correctly, it causes problems in the dimensional and planar surface control stages within both panels. Prior to the analysis process, the most suitable material first tried to select to prevent the process deformations. These materials contain general measurements determined in previous studies. During the analysis phase, operations performed according to the material properties shown in Table 1.

Table 1: Material properties.

Material	Modulus of elasticity, GPa	Poisson's ratio	Yield strength, MPa
AA6061-T6	66.6	0.33	276
AA6022-T4	70	0.33	250

Experiments were conducted for each of these materials in the LS-Dyna and Ls-Prepost analysis software, not for a portion of the body panels, but in the form of flat surface-smooth edge hemming. The purpose of this software is to use the previous studies in this direction. AA6022-T4 material found to be the most compatible in terms of strength, and the application took place with this material on a large scale.

In general, the materials are adapted to the robotic cylinder hemming process by referencing the previously determined material and work piece measurements in accordance with better product quality and less deformation on the operation surface. During the production of the left sliding door used, all important material and machine usage parameters specified. All of these operations shown on the short left sliding door work piece in the Ford v227 model. The finished product dimensions of the SWB model left sliding door L = 1040 mm and when considering the combined car body model, the gap of the door body frame G = 606 mm. The G value also considered as the width of the left sliding door.

For the robotic cylinder hemming process, creating a smooth outer panel surface quality identified as the primary goal. Although the operation we do affects the edge surface of the work pieces, we need a good fixture for the operation. As shown in Figure 2, a mold fixture designed for the hemming process where we placed the work piece on it.

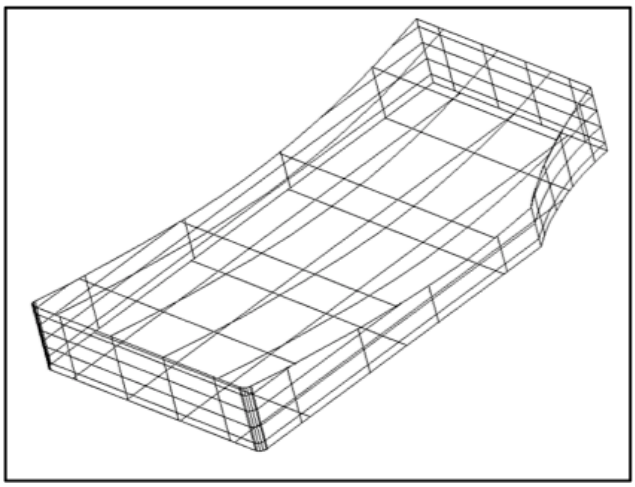

Figure 2. Robotic cylinder die fixture for hemming process.

All of these operations shown on the short left sliding door work piece in the Ford v227 model. The finished product dimensions of the SWB model left sliding door L value 1040 mm and when considering the combined car body model, the gap of the door body frame G value is 606 mm. The G value can also considered as the width of the left sliding door. For the robotic cylinder hemming process, creating a smooth outer panel surface quality identified as the primary goal. Although the operation we do affects the edge surface of the work pieces, we need a good fixture for the operation. A mold fixture designed where we placed the work piece on it for the hemming process.

The die fixture shown in Figure 2 designed independently of the traditional fixture and fixture jaws. The body is the same shape in accordance with the model. There is edge curves located at the bottom of the die fixture. This is because the most deformation seen in this region during the hemming process.
Figure 2 also provides external and internal panel Solidworks models. The dimensions of the die fixture have to be smaller than the outer panel of the body. This needed so that the roles on the outer panel edges can move along the robot's trajectory. In other words, it is necessary to avoid contact with the mold fixture and the robot Roller reel. If it not done in this way, deformation occurs on the outer panel and we damage the surface of the robot cylinder.
Based on the dimensions of the outer panel, two times the distance of the flange length that will occur during folding made inside. On this non-contact surface between the mold fixture and the outer panel will come the fixture jaws that connect to the mold. In this way, with the mold fixture used, the robot does not strike on the cylinder surface and deformations on the work piece also affected positively.
After the mold fixture, the outer panel, the most important factor determining the robotic cylinder hemming process, examined. The outer panel of the body is the part where the most deformation seen during and after the operation. Outer panel flat surface in appearance -flat edge, sloping surface-flat edge and sloping surface-it has a sloping edge structure. The study examined the deformation of these surfaces.
Another work piece that allows the outer panel to perform hemming is the inner panel. The inner panel is an important factor that forms the skeleton of the car door. It has a more detailed appearance structure than the outer panel (Figure 3).
In the inner panel there are records supporting the outer panel and details forming the glazed part. It is dimensionally smaller as it forms the hemming process by folding over the edges of the outer panel. Outer panel flange length and outer panel sheet thickness 2 times the total distance lengthened from the inside. As with the outer panel, it has a flat surface-flat edge, sloping surface-flat edge, and sloping surface - sloping edge structure.

All of these appearances drawn in Solidworks software and detailed by request of the manufacturer. These drawings then made for use in analysis software. First their analysis done in LS-Dyna and LS-Prepost software. Since the superficial accuracy of the process in material structure, node point and element selection was not trusted in LS-Dyna software, no comprehensive experimental results obtained. Second, LS-Prepost was preferred with parameters for printing, stamping and hemming, allowing analysis within the software.
The analysis process performed using the materials stated in the previous pages. The material thickness of the inner and outer panel first tested in accordance with the theses and papers made by the researchers.
For a single sheet with a flat surface-flat edge structure, deformations during the process experimentally analyzed for each material. Operations performed using 8-node solid and shell elements.
To obtain a 90° flange, AA6062-T4 material with optimal strength selected by calculating the strength, stress, and force of the applied cylinder.
Here 8-node solid elements preferred for the 1.2 mm thickness of the work piece. In the first place, no attention paid to the track surface measurements using sample parts. Analysis initiated by giving the robot cylinder a diameter of 25 mm. A lower die surface designed to test for deformations occurring on the work piece. In order to form the flange the corner of the work piece considered the reference point and the robot cylinder carried out a 90° hemming pre-flange operation in the edge trajectory (Figure 3). Changes shown on the flange surface in areas in close contact with the cylinder. Areas with maximum pre-tension shown in red. Von Mises pre-stress values for this process given.

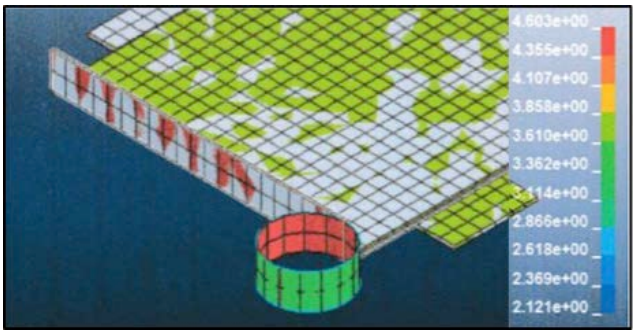

Figure 3. Hemming cylinder trajectory.

The improving the mesh value gives improved hemming cylinder trajectory (Figure 4).

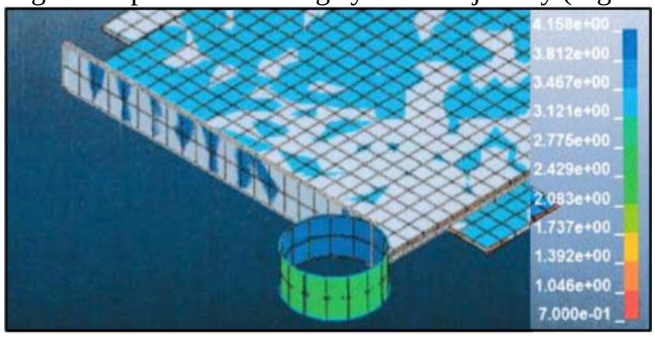

Figure 4. Improved hemming cylinder trajectory.

After this preliminary examination and improvements, new analyses made including the body inner panel and outer panel, mold fixture and robot cylinder. These analyses changes in surface quality and von Mises pre-stress ratio found (Figure 5).
These values applied to all edges of the body inner panel in LS-Prepost software. In other words, deformation analysis of flat surface-flat edge, sloping surface-flat edge and sloping surface-sloping edge structure performed.
During this analysis, inner panel and die fixture from other process elements are also included. Analysis was carried out so that the outer panel, inner panel, mold fixture and robot cylinder were in contact. The analysis again shown by hemming the 90° front flange to find the pre-stress values.

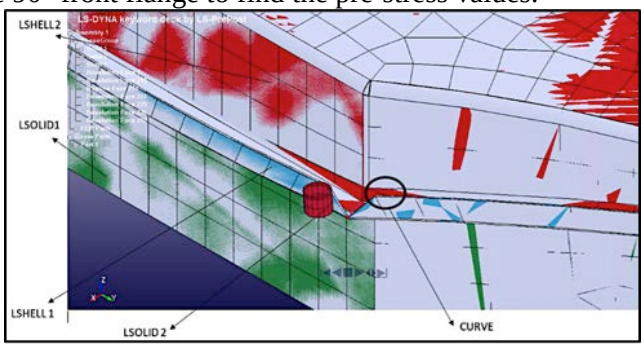

Figure 5. Hemming parts element structure of robotic cylinder.

In the team selection, the piece of ISOLID2I threw mesh selected. The material and values of the outer (LSHELL1) and inner (LSHELL2) panels given. The starting points of the flange section kept as work trajectory. As soon as selection translated to the cylinder shows its progress. Diameter 1.2 mm, gap 3 mm, rotation angle 45o, and displacement force in y direction 500 N determined.
Beyond this work, the PamStamp-2G software, which is currently preferred for the process of shaping sheet metal parts, was also used. Based on the data we obtained in LS-PrePost software, it done using the same data. The only difference between PamStamp-2G software and LS-Prepost software that one can enter the data of the cylinder that will do the hemming operation on the work piece in the prepared software. As shown in the Figure 6 the hemming front flange tension very is high at the edges of the sloping surface in the first attempt. The mesh values of the analysis and the anisotropy of the material on the work piece re-examined.

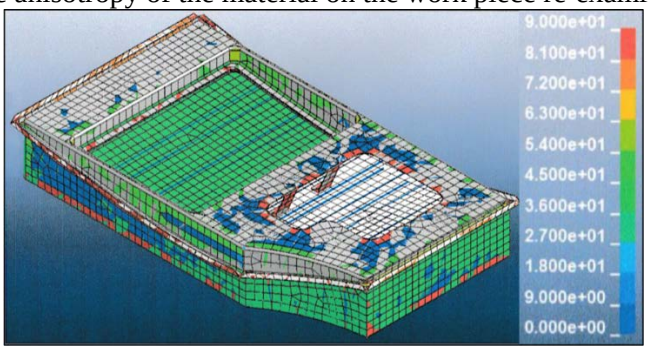

Figure 6. Deformation caused by force applied by hemming cylinder.

After these changes, the front tension rate of the outer panel during the front flange operation reduced. The Figure 7 shows the final pre-flange operation that occurred after the last trials.

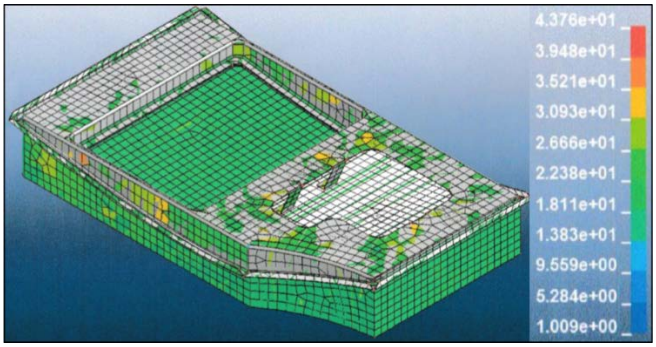

Figure 7. Improved deformation caused by the force applied by the hemming cylinder.

PamStamp-2G software panels and mold appearance given in Figure 8.

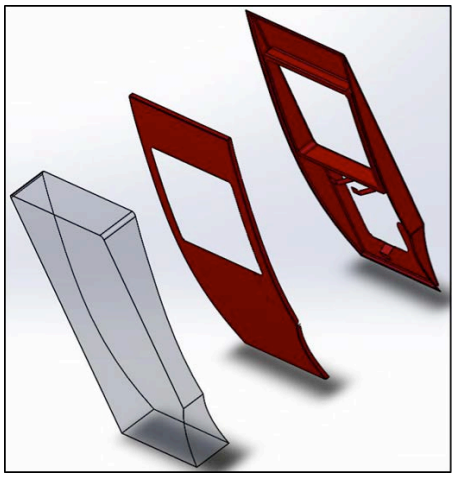

Figure 8. PamStamp-2G software panels and mold appearance.

To do the robotic cylinder hemming process, there a ready-made robot design courser. In this software, both front flange and final hemming performed. Because the values obtained are close to LS-prepare software, the data here not used. As a result operations the robotic cylinder hemming process shown in the following ways. In the first figure, surface deformation of the hemming cylinder advancing on the work panel trajectory shown. Deformation formed during hemming in rounded corners at the top of the outer panel shown.
The diagram shown in Figure 9 the elastic shape shifting of the AA6062-T4 aluminum material during the cylinder hemming process. The upper and lower flow limit of the material the part where deformation most observed.

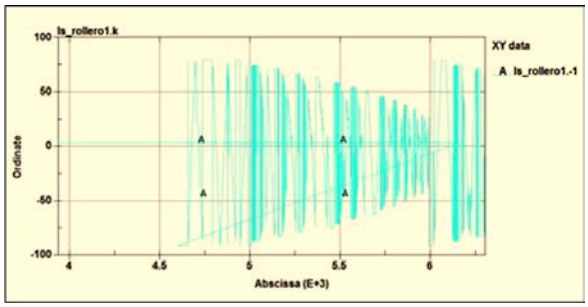

Figure 9. Surface deformation due to trajectory and hemming.

Luder formation occurs in the lower and upper part of the flow boundary. Here, this region, which forms the elastic shape-shifting part of the stress and deformation curve examined. The deformation at the rounded corner at the top of the outer panel leads to back flexing.

The deformation at critical mesh points at the coordinates y (ordinate) and x (abscissa) during the movement of the cylinder on the outer panel is shown in this way for the flange length of 12.4 mm. The flow limits low as the operation does not take place at the mesh points between 5.5 mm and 6 mm.

The A points shown on the y-axis in the diagram the center part of the flange length (0) and the edge of the panel (-50) indicating the yield strength limit formed by the cylinder on the surface. The vertex deformation explained in this diagram. This deformation occurred during the factory clinch process by converting the edges of the panel into a smooth edge structure in the drawing, i.e. by folding the edges on the edge surfaces created by breaking 45° chamfer instead of the rounded corner structure.

During the cylinder's trajectory, deformation increased as it reached critical areas. During the front flange, the crease on the panel edge corrected with final hemming. The final hemming of the front flange, which made with a cylinder diameter of 25 mm, with a cylinder diameter of 40 mm immediately following, removed the crumpling. In addition, the force increased to 650 N, preventing back stretching and reducing the surface roughness rate to a minimum.

In Figure 10, the stress generated by the trajectory cylinder in the outer panel shown. Where A is the expression of the stress resistance shown by each step of the cylinder on the trajectory at the mesh points. A stable uplift observed at each step in critical areas of the sloping edge.

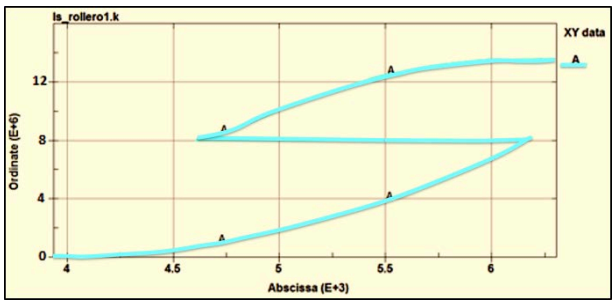

Figure 10. Trajectory and pre-stress resulting from hemming step.

Analysis diagram, at a certain mesh distance of the surface on the x-axis and 12.4 mm on the y-axis the flange consists of a change in shape that occurs on the neck. At the critical mesh points on the x-axis, the displacement on the mesh surface of 0 to 6 mm shown. For material AA6062-T4, the region where the stress stable between points A's. Result of the force applied on this material, which is ductile and under the general yield limit shows

low shape shifting behavior. Flange seen flexing back on the neck. Critical mesh points on the x-axis, the stresses and strains with a displacement force of 650 N on the 4.6 to 6.6 mm mesh surface shown in High strength and toughness behavior seen of the new force applied on this material, which ductile and tension above the yield limit. On the flange length surface, back flexing prevented at a distance of 8 mm and 12.4 mm. Finally, the surface hardness strength of the AA6062-T4 material examined. The analysis diagram shows the surface hardness, which occurs at a certain mesh distance of the surface at the x-axis and at a flange length of 12.4 mm at the y-axis (Figure 11).

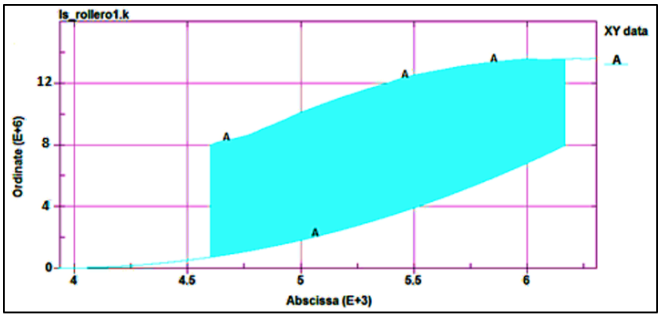

Figure 11. Surface hardness values of the material AA6062-T4.

At critical mesh points on the x-axis, the tensile and surface hardness formed by the displacement force of 500 N shown. Point A for material AA6062-T4 the only region where surface hardness seen.
Since the force cannot complete the shape-shifting behavior on the surface without stretching back, it makes contact with a single point of strength at surface hardness. Therefore, no change seen on a large scale.
Stress and surface hardness resistance formed by 650 N displacement force, on 4.6 mm to 6.6 mm mesh surface at critical mesh points on the x-axis shown. Result of the new force applied on this material, which is ductile and tension above the yield limit, high surface hardness resistance seen at three points. Wrinkle, tear, etc. in aluminum alloys where deformations occur, 6022 - T4E32 found to have the best material properties.

4. Results and Discussion

The aim of this study is to show that the steps of hemming, mastic and laser curing process proceed in a complementary manner with the robot arm attached to a single robot. In order to perform these complementary steps, some parameters that also affect process quality need to be determined. The effects of the placement of the robot arm on the work piece analyzed numerically and the optimal processing parameters were determined. The nets are refined to a minimum size of 0.2 mm. The flange area is the folding area. The Nets are refined to a minimum size of 1 mm. The transition and very slightly deformed regions are rough-knit. Ultimately, there are 17,956 elements anointed to the outer space. While the inner cavity roughly knitted into the rough, the cylinder slightly deformed during the hemming process.

In the team selection, the piece of ISOLID2I threw mesh selected. The material and values of the outer (LSHELL1) and inner (LSHELL2) panels given. The starting points of the flange section kept as work trajectory. As soon as selection translated to the cylinder shows its progress.

The deformation at critical mesh points at the coordinates y (ordinate) and x (abscissa) during the movement of the cylinder on the outer panel is shown in this way for the flange length of 12.4 mm. The flow limits low as the operation does not take place at the mesh points between 5.5 mm and 6 mm.

Result of the force applied on this material, which is ductile and under the general yield limit shows low shape shifting behavior. Flange seen flexing back on the neck. Critical mesh points on the x-axis, the stresses and strains with a displacement force of 650 N on the 4.6 to 6.6 mm mesh surface shown in High strength and toughness behavior seen of the new force applied on this material, which ductile and tension above the yield limit.
Wrinkle, tear, etc. in aluminum alloys where deformations occur, 6022 - T4E32 found to have the best material properties.

5. Results and Discussion

The effects of the placement of the robot arm on the work piece analyzed numerically and the optimal processing parameters were determined. The nets are refined to a minimum size of 0.2 mm. The flange area is the folding area. The Nets are refined to a minimum size of 1 mm. The transition and very slightly deformed regions are rough-knit. Ultimately, there are 17,956 elements anointed to the outer space. While the inner cavity roughly knitted into the rough, the cylinder slightly deformed during the hemming process. The deformation at critical mesh points at the coordinates y (ordinate) and x (abscissa) during the movement of the cylinder on the outer panel is shown in this way for the flange length of 12.4 mm. Wrinkle, tear, etc. in aluminum alloys where deformations occur, 6022 - T4E32 found to have the best material properties.

References

[1] Toeniskoetter JB. Roller hemming machine. US Patent USOO7124611B2 (12) (10) Patent No.: US 7,124,611 B2, Oct. 24, 2006.

[2] Toeniskoetter JB. Rollertype hemming apparatus. US Patent US007 152447B2 (10) Patent No.: US 7,152.447 B2 Dec. 26, 2006.

[3] Le Maout N, Manach PY, Pauvert O, Thuillier S. 2008, numerical simulation of the hemming process - integration in the virtual design of automotive parts. Numisheet 2008;1-5:699-704.

[4] Le Maout N, Thuillier S, Manach PY. Aluminum alloy damage evolution for different strain paths–Application to hemming process. Eng Fracture Mech 2009;76:1202-1214.

[5] Muderrisoglu A, Murata M, Ahmetoglu MA, Kinzel G, Altan T. Bending, flanging, and hemming of aluminum sheet—an experimental study. J Mater Process Technol 1996;59:10–7.

[6] Zhang G, Wu X, Hu SJ. A study on fundamental mechanisms of warp and recoil in hemming. J Eng Mater Technol 2001;123:436–441.

[7] Zhang, G, Hao, H, Wu X, Hu SJ, Harper K, Faite W. An experimental investigation of curved surface-straight edge hemming. J Manufacturing Processes 2000;4:241-246.

[8] Livatyali H, Müderrisoğlu A, Ahmetoğlu M, Akgerman N, Kinzel G, Altan T. Improvement of hem quality by optimizing flanging and pre-hemming operations using computer aided die design. J Mater Process Technol 2000;98:41–52.

[9] Bagheri F, Madoliat R, Sedighi M, Asgari A. Rubber-assisted pre-hemming process: A parametric study. J Manufacturing Processes 2019; 38:328–337.

[10] Kolahdooz R, Asghari S, Rashid-Nadimi S, Amirfazli A. Integration of finite element analysis and design of experiment for the investigation of critical factors in rubber pad forming of metallic bipolar plates for PEM fuel cells. Int J Hydrogen Energy 2017;42:575–89.

[11] Lin G. Quality and formability in hemming of automotive aluminum alloys. ProQuest Disertation and Theses (PQDT) 2006.

[12] Lin, G., Li, J., Hu, S. J., Cai, W., A Computational Response Surface Study of Three-Dimensional Aluminum Hemming Using Solid-to-Shell Mapping, Journal of Manufacturing Science and Engineering, Vol. 129, April 2007, 360-368.

[13] Le Port A, Thuillier S, Manach PY. Characterization of surface defects after flanging of metallic sheets. J Mater Process Technol 2011;211:2062–71.

[14] Sasso M, Palmieri G, Chiappini G, Amodio D. Characterization of hyperelastic rubber-like materials by biaxial and uniaxial stretching tests based on optical methods. Polym Test 2008;27:995–1004.

[15] Lee J, Bong HJ, Ha J, Choi J, Barlat F, Lee MG. Influence of yield stress determination in anisotropic hardening model on springback prediction in dual-phase steel. JOM 2018;70:1560–6.

[16] Wanintradul C, Golovashchenko SF, Gillard AJ, Smith LM. Hemming process with counteraction force to prevent creepage. J Manuf Process 2014;16:379–90.

[17] Zhang G, Wu X, Hu SJ. A study on fundamental mechanisms of warp and recoil in hemming. J Eng Mater Technol 2001;123:436–441.

[18] Thuillier S, Le Maoût N, Manach PY, Debois D. Numerical simulation of the roll hemming process. J Mater Process Tech 2008;198:226-233.